AIAA 81-4131

Vibration of a Materially Monoclinic, Thick-Wall Circular Cylindrical Shell

M. E. Vanderpool*
General Dynamics Corp., Fort Worth, Texas
and
C. W. Bert†
University of Oklahoma, Norman, Okla.

The resonant vibration frequencies of a fiber-reinforced, thick-wall, circular-cylindrical shell of finite length which is materially monoclinic are analyzed. The degree of material anisotropy precludes a closed-form solution and so an iterative, yet exact, method is used. The analytical method is validated by comparison of results with previously published results for a homogeneous, isotropic thin shell, and an orthogonally stiffened-thin shell modeled as orthotropic. Results for a materially monoclinic, thick-wall shell with free-free end conditions are compared with experimental results obtained by the present investigators.

Nomenclature

$[A^k]$	= matrices defined in Appendix D of Ref. 8
$[B^k]$	= matrices defined in Eqs. (18)
C_{ij}	= stiffness matrix coefficients
$[D]$	= lambda matrix defined in Eq. (15)
E_f, E_m	= Young's moduli of fiber and matrix
E_i	= orthotropic Young's modulus in material-symmetry direction i
G_f, G_m	= shear moduli of fiber and matrix
G_{ij}	= orthotropic shear modulus with respect to material-symmetry axes i and j
h	= shell thickness
$[I]$	= identity matrix
i	$= \sqrt{-1}$
i,j	= indices (1,...,6) or (x,θ,z)
k	= index (1,...,10)
ℓ	= shell length
M_{ij}	= moment resultants
N_{ij}	= in-surface stress resultants
n	= circumferential wave number
Q_i	= thickness-shear stress resultants
R	= mean radius of shell
S_{ij}	= elastic compliances
t	= time
u, v, w	= middle-surface displacements in directions x, θ, z, respectively
$\bar{u}, \bar{v}, \bar{w}$	= displacements in directions x, θ, z, respectively
U, V, W	= amplitudes of u, v, w,
V_f, V_m	= fiber and matrix volume fractions
x, z	= coordinates in axial and radial directions, respectively
$[Z]$	= matrix defined in Eq. (17)
$\bar{\alpha}, \bar{\beta}, \bar{\eta}$	= constant values of integrals
$\epsilon_{ij}, \gamma_{ij}$	= normal and shear strain components
θ	= circumferential angular-position coordinate
λ	= axial wave parameter
κ^2	= shear correction factor
ν_f, ν_m	= Poisson's ratios of fiber and matrix
ν_{ij}	= orthotropic Poisson's ratio, unit contraction in direction j per unit extension in direction i, due to uniaxial tension in direction i
ρ	= density
σ_{ij}, τ_{ij}	= normal and shear stress components
ψ, ϕ	= bending slopes
Ψ, Φ	= amplitudes of ψ and ϕ, respectively
ω	= angular frequency
$(\ )_{,x\theta}$	$= \partial^2(\ )/\partial x \partial\theta$

I. Introduction

DETERMINATION of the free-vibration characteristics of cylindrical shells continues to be a problem of great interest to engineers. The subject has application in many fields, especially the structural dynamics of aircraft, missiles, space vehicles, and ocean vehicles. It is, in great part, for these same applications that the recent interest in filamentary composites is so high.

Most of the work on shell vibrations has dealt with those that are homogeneous and isotropic, and information for nonhomogeneous and anisotropic shells is limited. The voluminous literature on the subject was very ably summarized in Leissa's monograph.[1] There are also recent surveys on composite shell vibrations.[2,3] By far, the majority of the analyses found in the literature concerns shells that have a small thickness-to-radius ratio (<0.1). As a consequence of the thickness range, simplifying assumptions can often be made concerning stresses and strains in the thickness direction. Typical is Love's first approximation,[4] the analog to the Bernoulli-Euler beam theory, in which it is assumed that there is negligible warping in the thickness planes and that, hence, there is negligible thickness-shear strain. It is also assumed that thickness-normal stresses are negligible.

In dealing with filamentary composites, the notions of thickness and negligible warping must take on new meaning because of their inherent anisotropy and comparatively low-shear moduli.

In the present analysis, we consider the vibration of shells that can be very general in material nature, except that layered and sandwich types are excluded. They may be isotropic, specially orthotropic or monoclinic. A specially orthotropic shell is one that has three mutually perpendicular planes of symmetry and is exemplified by a fibrous composite in which the fibers are oriented either circumferentially or axially, Figs. 1a and 1b. Mirsky[5] analyzed the vibration problem for an infinitely long, specially orthotropic shell and included the

Received Jan. 7, 1980; revision received Oct. 6, 1980.

*Design Engineer, Fuselage Design Group.

†Benjamin H. Perkinson Professor of Engineering, School of Aerospace, Mechanical and Nuclear Engineering. Associate Fellow AIAA.

effects of thickness-shear flexibility, thickness-normal strain, and rotatory inertia.

A materially monoclinic shell has one less plane of symmetry than a specially orthotropic one. It may be characterized by an off-axis helical-wound construction, Fig. 1c. Generally, the term helical-wound refers to a doubly-wound (bi-helical) shell, but in the present context we mean a single direction. The material properties for a monoclinic shell are derived from a specially orthotropic one by a rotation of axes about a normal to the shell surface. In the present analysis, we investigate the vibration characteristics of the monoclinic shell, as it is the extreme practical case because of the complex coupling between in-surface normal and shear actions.

As in Mirsky's analysis, thickness-shear strain and rotatory inertia are included, but thickness-normal strain is neglected. An exact, but iterative, technique as suggested by Flügge in 1934 and later used by Forsberg[6] is employed. This technique permits general boundary conditions to be considered. The calculations were carried out on an IBM 370, Model 158J, high-speed, digital computer and results are compared with experimental results.

To the best knowledge of the present investigators, this is the first such analysis in which the techniques mentioned are applied to a finite-length, thick-wall shell of this material complexity.

II. Basic Equations

The equations given in this section require lengthy development which may be found in many books and papers on the subject of circular cylindrical shells.[1,7]

Hypotheses

The following assumptions are made concerning the description of the shell motion.[8]

1) The displacement components vary linearly across the thickness of the shell except for the radial component, w, which is constant for fixed x,θ, and t; i.e., a thickness-shear-flexible theory is used.

2) Displacements are small compared to the shell thickness so that the strain-displacement relations may be taken as linear.

3) The shell material is linearly elastic and macroscopically homogeneous and may be monoclinic, orthotropic, transversely isotropic, or isotropic, as desired.

4) The shell is circular cylindrical with a uniform wall thickness, which may be moderately thick.

5) Body forces and body moments are negligible.

6) Dissipative effects, such as damping, are negligible.

7) Acoustic fluid interactions are neglected, i.e., the shell is assumed to be vibrating in a vacuum.

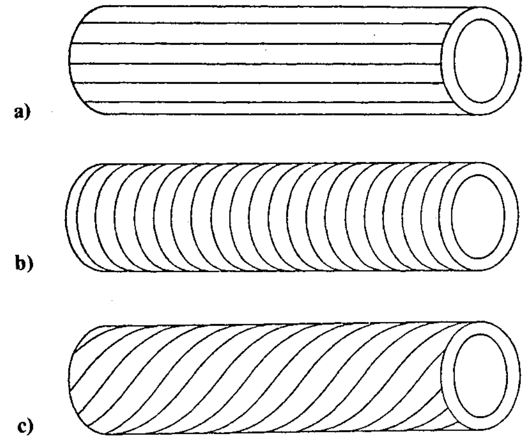

Fig. 1 Examples of specially orthotropic (a) and (b) and monoclinic (c) fiber orientations.

Equations of Motion

It has been shown[9] that the displacement components can be accurately approximated by the relations

$$\bar{u}(x,\theta,z,t) \approx u(x,\theta,t) + z\psi(x,\theta,t)$$

$$\bar{v}(x,\theta,z,t) \approx v(x,\theta,t) + z\phi(x,\theta,t)$$

$$\bar{w}(x,\theta,z,t) \approx w(x,\theta,t) \qquad (1)$$

where the axial and circumferential displacement distributions are linear across the shell thickness and the radial displacement is independent of the z coordinate. The result, then, is a linear shear-strain distribution and neglect of thickness-normal strain.

The five resulting equations of motion in terms of stress resultants become (Appendix A of Ref. 8):

$$N_{xx,x} + R^{-1}N_{\theta x,\theta} = \rho h[u_{,tt} + (h^2/12R)\psi_{,tt}]$$

$$N_{x\theta,x} + R^{-1}N_{\theta\theta,\theta} + R^{-1}Q_\theta = \rho h[v_{,tt} + (h^2/12R)\phi_{,tt}]$$

$$Q_{x,x} + R^{-1}Q_{\theta,\theta} - R^{-1}N_{\theta\theta} = \rho h[w_{,tt}]$$

$$M_{xx,x} + R^{-1}M_{\theta x,\theta} - Q_x = \rho(h^3/12)[\psi_{,tt} + R^{-1}u_{,tt}]$$

$$M_{x\theta,x} + R^{-1}M_{\theta\theta,\theta} - N_{z\theta} + R^{-1}M_{\theta z} = \rho(h^3/12)[\phi_{,tt} + R^{-1}v_{,tt}] \qquad (2)$$

where body forces and body moments have been neglected and rotatory inertia terms have been included. A comma preceding a coordinate variable indicates differentiation with respect to that variable.

The stress and moment resultants are obtained by integrating through the shell thickness using the following definitions.

$$(N_{xx},Q_x,N_{x\theta},N_{z\theta}) = \int_{-h/2}^{h/2} (\sigma_{xx},\tau_{xz},\tau_{x\theta},\tau_{z\theta})(1+R^{-1}z)\,dz$$

$$(N_{\theta\theta},N_{\theta x},Q_\theta) = \int_{-h/2}^{h/2} (\sigma_{\theta\theta},\tau_{x\theta},\tau_{z\theta})\,dz$$

$$(M_{xx},M_{x\theta}) = \int_{-h/2}^{h/2} (\sigma_{xx},\tau_{x\theta})(1+R^{-1}z)z\,dz$$

$$(M_{\theta\theta},M_{\theta x},M_{\theta z}) = \int_{-h/2}^{h/2} (\sigma_{\theta\theta},\tau_{x\theta},\tau_{z\theta})z\,dz \qquad (3)$$

It is noted that even though the stress tensor is symmetric, the stress resultants are not; i.e., $N_{x\theta} \neq N_{\theta x}$. If the shell is sufficiently thin, however, $R^{-1}z$ can often be neglected in comparison to 1; then the resultants will be symmetric. Such a simplification is not made here.

At this point, the constitutive relations expressing the stresses as linear functions of the strain components are employed. Since the filaments are wound helically along the shell length, the system is described as materially monoclinic with respect to cylindrical coordinates and has the following stress-strain relation.

$$\begin{Bmatrix} \sigma_{xx} \\ \sigma_{\theta\theta} \\ \sigma_{zz} \\ \tau_{xz} \\ \tau_{\theta z} \\ \tau_{x\theta} \end{Bmatrix} = \begin{bmatrix} C_{11} & C_{12} & C_{13} & 0 & 0 & C_{16} \\ C_{12} & C_{22} & C_{23} & 0 & 0 & C_{26} \\ C_{13} & C_{23} & C_{33} & 0 & 0 & C_{36} \\ 0 & 0 & 0 & C_{44} & C_{45} & 0 \\ 0 & 0 & 0 & C_{45} & C_{55} & 0 \\ C_{16} & C_{26} & C_{36} & 0 & 0 & C_{66} \end{bmatrix} \begin{Bmatrix} \epsilon_{xx} \\ \epsilon_{\theta\theta} \\ \epsilon_{zz} \\ \gamma_{xz} \\ \gamma_{\theta z} \\ \gamma_{x\theta} \end{Bmatrix} \qquad (4)$$

The components of the stiffness matrix are first derived for an orthotropic system, see Appendix B of Ref. 8, wherein the terms C_{16}, C_{26}, C_{36}, and C_{45} do not appear. A rotation about the z axis is then performed, bringing the matrix to the above form.

The well-known strain-displacement relations in cylindrical coordinates are

$$\epsilon_{xx}=\bar{u}_{,x};\ \epsilon_{\theta\theta}=(\bar{w}+\bar{v}_{,\theta})/(R+z);\ \epsilon_{zz}=\bar{w}_{,z};\quad \gamma_{x\theta}=\bar{v}_{,x}+[\bar{u}_{,\theta}/(R+z)];\ \gamma_{xz}=\bar{u}_{,z}+\bar{w}_{,x};\quad \gamma_{\theta z}=\bar{v}_{,z}+(\bar{w}_{,\theta}-\bar{v})/(R+z) \tag{5}$$

Here the small-displacement assumption permits omission of all nonlinear terms.

Substituting Eqs. (1) into Eqs. (5) results in

$$\epsilon_{xx}=u_{,x}+z\psi_{,x};\ \epsilon_{\theta\theta}=(w+v_{,\theta}+z\phi_{,\theta})/(R+z);\ \epsilon_{zz}=0;\quad \gamma_{x\theta}=v_{,x}+z\phi_{,x}+(u_{,\theta}+z\psi_{,\theta})/(R+z)$$

$$\gamma_{xz}=\psi+w_{,x};\ \gamma_{\theta z}=\phi+(w_{,\theta}-v-z\phi)/(R+z) \tag{6}$$

To get the equations of motion, Eqs. (2), in terms of displacement components only, we substitute Eqs. (6) into Eqs. (4), calculate the resultants in Eqs. (3), and finally substitute the result into Eqs. (2).

Most shell theories, including the one used here, are strictly two-dimensional theories which provide for only a linear distribution of thickness shear deformation over the shell thickness. Since the thickness shear deformation is approximately quadratic in the thickness coordinate, we introduce a correction factor to account for the discrepancy. Mindlin[10] showed that for a vibrating plate, homogeneous through the thickness, the thickness-shear motion correction factor can be taken as

$$\kappa^2=\pi^2/12 \tag{7}$$

Hence, we multiply the terms containing the shear strains γ_{xz} and $\gamma_{\theta z}$ by κ^2 prior to evaluating the resultants in Eqs. (3).

It is convenient at this point to define the following integral constants for use in evaluating Eqs. (3).[11]

$$\bar{\alpha}=\int_{-h/2}^{h/2}\mathrm{d}z/(R+z)=\ln\left[\frac{1+(h/2R)}{1-(h/2R)}\right]\qquad \bar{\beta}=\int_{-h/2}^{h/2}z\mathrm{d}z/(R+z)=h\left\{1-\frac{R}{h}\ln\left[\frac{1+(h/2R)}{1-(h/2R)}\right]\right\}=h-R\bar{\alpha}$$

$$\bar{\eta}=\int_{-h/2}^{h/2}z^2\mathrm{d}z/(R+z)=-Rh\left\{1-\frac{R}{h}\ln\left[\frac{1+(h/2R)}{1-(h/2R)}\right]\right\}=R^2\bar{\alpha}-Rh \tag{8}$$

The resulting equations of motion in terms of displacement components become

$$C_{11}hu_{,xx}+2C_{16}\frac{h}{R}u_{,\theta x}+C_{66}\frac{\bar{\alpha}}{R}u_{,\theta\theta}+C_{16}hv_{,xx}+(C_{12}+C_{66})\frac{h}{R}v_{,\theta x}+C_{26}\frac{\bar{\alpha}}{R}v_{,\theta\theta}+C_{12}\frac{h}{R}w_{,x}+C_{26}\frac{\bar{\alpha}}{R}w_{,\theta}+C_{11}\frac{h^3}{12R}\psi_{,xx}$$
$$+C_{66}\frac{\bar{\beta}}{R}\psi_{,\theta\theta}+C_{16}\frac{h^3}{12R}\phi_{,xx}+C_{26}\frac{\bar{\beta}}{R}\phi_{,\theta\theta}=\rho h\left(u_{,tt}+\frac{h^2}{12R}\psi_{,tt}\right) \tag{9a}$$

$$C_{16}hu_{,xx}+(C_{12}+C_{66})\frac{h}{R}u_{,\theta x}+C_{26}\frac{\bar{\alpha}}{R}u_{,\theta\theta}+C_{66}hv_{,xx}+2C_{26}\frac{h}{R}v_{,\theta x}+C_{22}\frac{\bar{\alpha}}{R}v_{,\theta\theta}-\kappa^2C_{55}\frac{\bar{\alpha}}{R}v+\left(C_{26}+\kappa^2C_{45}\frac{h}{R}\right)w_{,x}$$
$$+(C_{22}+\kappa^2C_{55})\frac{\bar{\alpha}}{R}w_{,\theta}+C_{16}\frac{h^3}{12R}\psi_{,xx}+C_{26}\frac{\bar{\beta}}{R}\psi_{,\theta\theta}+\kappa^2C_{45}\frac{h}{R}\psi+C_{66}\frac{h^3}{12R}\phi_{,xx}+C_{22}\frac{\bar{\beta}}{R}\phi_{,\theta\theta}+\kappa^2C_{55}\left(\frac{h-\bar{\beta}}{R}\right)\phi$$
$$=\rho h\left(v_{,tt}+\frac{h^2}{12R}\phi_{,tt}\right) \tag{9b}$$

$$-C_{12}\frac{h}{R}u_{,x}-C_{26}\frac{\bar{\alpha}}{R}u_{,\theta}-(-\kappa^2C_{45}+C_{26})\frac{h}{R}v_{,x}-(C_{22}+\kappa^2C_{55})\frac{\bar{\alpha}}{R}v_{,\theta}+\kappa^2C_{44}hw_{,xx}+2\kappa^2C_{45}\frac{h}{R}w_{,x\theta}+\kappa^2C_{55}\frac{\bar{\alpha}}{R}w_{,\theta\theta}$$
$$-C_{22}\frac{\bar{\alpha}}{R}w+\kappa^2C_{44}h\psi_{,x}+\left(\kappa^2C_{45}\frac{h}{R}-C_{26}\frac{\bar{\beta}}{R}\right)\psi_{,\theta}+\kappa^2C_{45}h\phi_{,x}+\left[\kappa^2C_{55}\frac{h}{R}-(C_{22}+\kappa^2C_{55})\frac{\bar{\beta}}{R}\right]\phi_{,\theta}=\rho hw_{,tt} \tag{9c}$$

$$C_{11}\frac{h^3}{12R}u_{,xx}+C_{66}\frac{\bar{\beta}}{R}u_{,\theta\theta}+C_{16}\frac{h^3}{12R}v_{,xx}+C_{26}\frac{\bar{\beta}}{R}v_{,\theta\theta}+\kappa^2C_{45}\frac{h}{R}v-\kappa^2C_{44}hw_{,x}+\left(C_{26}\frac{\bar{\beta}}{R}-\kappa^2C_{45}\frac{h}{R}\right)w_{,\theta}+C_{11}\frac{h^3}{12}\psi_{,xx}$$
$$+2C_{16}\frac{h^3}{12R}\psi_{,\theta x}+C_{66}\frac{\bar{\eta}}{R}\psi_{,\theta\theta}-\kappa^2C_{44}h\psi+C_{16}\frac{h^3}{12}\phi_{,xx}+(C_{12}+C_{66})\frac{h^3}{12R}\phi_{,\theta x}+C_{26}\frac{\bar{\eta}}{R}\phi_{,\theta\theta}-\kappa^2C_{45}h\phi=\rho\frac{h^3}{12}\left(\psi_{,tt}+\frac{1}{R}u_{,tt}\right) \tag{9d}$$

$$C_{16}\frac{h^3}{12R}u_{,xx}+C_{26}\frac{\bar{\beta}}{R}u_{,\theta\theta}+C_{66}\frac{h^3}{12R}v_{,xx}+C_{22}\frac{\bar{\beta}}{R}v_{,\theta\theta}+\kappa^2C_{55}\left(\frac{h-\bar{\beta}}{R}\right)v-\kappa^2C_{45}hw_{,x}+\left[C_{22}\frac{\bar{\beta}}{R}-\kappa^2C_{55}\left(\frac{h-\bar{\beta}}{R}\right)\right]w_{,\theta}$$

$$+C_{16}\frac{h^3}{12}\psi_{,xx}+(C_{12}+C_{66})\frac{h^3}{12R}\psi_{,\theta x}+C_{26}\frac{\bar{\eta}}{R}\psi_{,\theta\theta}-\kappa^2C_{45}h_\psi+C_{66}\frac{h^3}{12}\phi_{,xx}+C_{22}\frac{\bar{\eta}}{R}\phi_{,\theta\theta}-\kappa^2C_{55}\left(\frac{h+\bar{\eta}}{R}\right)=\rho\frac{h^3}{12}\left(\phi_{,tt}+\frac{1}{R}v_{,tt}\right) \quad (9e)$$

Boundary Conditions

The method of analysis is general enough to be used with any desired boundary conditions at the ends, $x=0,\ \ell$. For comparison with experimental results, the free-free condition‡ was chosen, as it was the easiest to obtain in the laboratory. Accordingly, we have the following free-free conditions at $x=0$ and $x=\ell$.

$$N_{xx}=0;\quad N_{x\theta}=0;\quad Q_x=0;\quad M_{xx}=0;\quad M_{x\theta}=0 \quad (10)$$

In terms of displacement components, we proceed as before and obtain

$$C_{11}hu_{,x}+C_{16}\frac{h}{R}u_{,\theta}+C_{16}hv_{,x}+C_{12}\frac{h}{R}v_{,\theta}+C_{12}\frac{h}{R}w+C_{11}\frac{h^3}{12R}\psi_{,x}+C_{16}\frac{h^3}{12R}\phi_{,x}=0 \text{ at } x=0,\ \ell \quad (11a)$$

$$C_{16}hu_{,x}+C_{66}\frac{h}{R}u_{,\theta}+C_{66}hv_{,x}+C_{26}\frac{h}{R}v_{,\theta}+C_{26}\frac{h}{R}w+C_{16}\frac{h^3}{12R}\psi_{,x}+C_{66}\frac{h^3}{12R}\phi_{,x}=0 \text{ at } x=0,\ \ell \quad (11b)$$

$$-\kappa^2C_{45}\frac{h}{R}v+\kappa^2C_{44}hw_{,x}+\kappa^2C_{45}\frac{h}{R}w_{,\theta}+\kappa^2C_{44}h\psi+\kappa^2C_{45}h\phi=0 \text{ at } x=0,\ \ell \quad (11c)$$

$$C_{11}\frac{h^3}{12R}u_{,x}+C_{16}\frac{h^3}{12R}v_{,x}+C_{11}\frac{h^3}{12}\psi_{,x}+C_{16}\frac{h^3}{12R}\psi_{,\theta}+C_{16}\frac{h^3}{12}\phi_{,x}+C_{12}\frac{h^3}{12R}\phi_{,\theta}=0 \text{ at } x=0,\ \ell \quad (11d)$$

$$C_{16}\frac{h^3}{12R}u_{,x}+C_{66}\frac{h^3}{12R}v_{,x}+C_{16}\frac{h^3}{12}\psi_{,x}+C_{66}\frac{h^3}{12R}\psi_{,\theta}+C_{66}\frac{h^3}{12}\phi_{,x}+C_{26}\frac{h^3}{12R}\phi_{,\theta}=0 \text{ at } x=0,\ \ell \quad (11e)$$

III. Method of Analysis

Since the object of the present analysis is to predict resonant frequencies, the solutions of the equations of motion, Eqs. (9), and the boundary conditions, Eqs. (11), are assumed to be harmonic functions in a so-called semi-inverse method. The procedure follows closely that suggested by Flügge [12] and demonstrated by Forsberg [6] for thin isotropic shells.

Assumed Displacements

Because of the materially anisotropic nature of the shell in the present analysis, care must be exercised in selecting the displacement functions. The primary difficulty encountered here is readily seen in the various combinations of odd and even derivatives in the equations of motion. The amplitudes, U, V, W, Ψ, and Φ given in Eqs. (12) below are, in general, complex numbers. Noticing that, in Eqs. (9), each equation either contains an even or odd number of differentiations of each displacement component, but not both even and odd, we conveniently assume

$$u=U\exp\left[i\left(\frac{\lambda x}{\ell}+n\theta-\omega t\right)\right],\quad v=V\exp\left[i\left(\frac{\lambda x}{\ell}+n\theta-\omega t\right)\right]$$

$$w=iW\exp\left[i\left(\frac{\lambda x}{\ell}+n\theta-\omega t\right)\right],\quad \psi=\Psi\exp\left[i\left(\frac{\lambda x}{\ell}+n\theta-\omega t\right)\right],\quad \phi=\Phi\exp\left[i\left(\frac{\lambda x}{\ell}+n\theta-\omega t\right)\right] \quad (12)$$

Substituting Eqs. (12) into Eqs. (9) and carrying out the differentiations, we obtain the following equations of motion.

$$\left[-C_{11}\frac{h}{\ell^2}\lambda^2-2C_{16}\frac{hn}{R\ell}\lambda-C_{66}\frac{\bar{\alpha}n^2}{R}+\rho h\omega^2\right]U+\left[-C_{16}\frac{h}{\ell^2}\lambda^2-(C_{12}+C_{66})\frac{hn}{R\ell}\lambda-C_{26}\frac{\bar{\alpha}n^2}{R}\right]V$$

$$+\left[-C_{12}\frac{h}{R\ell}\lambda-C_{26}\frac{\bar{\alpha}n}{R}\right]W+\left[-C_{11}\frac{h^2}{12R\ell^2}\lambda^2-C_{66}\frac{\bar{\beta}n^2}{Rh}+\rho\frac{h^2\omega^2}{12R}\right]h\Psi+\left[-C_{16}\frac{h^2}{12R\ell^2}\lambda^2-C_{26}\frac{\bar{\beta}n^2}{Rh}\right]h\Phi=0 \quad (13a)$$

$$\left[-C_{16}\frac{h}{\ell^2}\lambda^2-(C_{12}+C_{66})\frac{hn}{R\ell}\lambda-C_{26}\frac{\bar{\alpha}n^2}{R}\right]U+\left[-C_{66}\frac{h}{\ell^2}\lambda^2-2C_{26}\frac{hn}{R\ell}\lambda-C_{22}\frac{\bar{\alpha}n^2}{R}-\kappa^2C_{55}\frac{\bar{\alpha}}{R}+\rho h\omega^2\right]V$$

$$+\left[-(C_{26}+\kappa^2C_{45})\frac{h}{R\ell}\lambda-(C_{22}+\kappa^2C_{55})\frac{\bar{\alpha}n}{R}\right]W+\left[-C_{16}\frac{h^2}{12R\ell^2}\lambda^2-C_{26}\frac{\bar{\beta}n^2}{Rh}+\kappa^2C_{45}\frac{1}{R}\right]h\Psi$$

$$+\left[-C_{66}\frac{h^2}{12R\ell^2}\lambda^2-C_{22}\frac{\bar{\beta}n^2}{Rh}-\kappa^2C_{55}\frac{\bar{\beta}}{Rh}+\kappa^2C_{55}\frac{1}{R}+\rho\frac{h^2\omega^2}{12R}\right]h\Phi=0 \quad (13b)$$

‡The program, Appendix E of Ref. 8, is designed to handle any homogeneous end condition.

$$\left[-C_{12}\frac{h}{R\ell}\lambda - C_{26}\frac{\bar{\alpha}n}{R} + \rho\frac{h^3\omega^2}{12R}\right]U + \left[-(C_{26}+\kappa^2C_{45})\frac{h}{R\ell}\lambda - (C_{22}+\kappa^2C_{55})\frac{\bar{\alpha}n}{R}\right]V$$
$$+\left[-\kappa^2C_{44}\frac{h}{\ell^2}\lambda^2 - 2\kappa^2C_{45}(hn/R\ell)\lambda - \kappa^2C_{55}\frac{\bar{\alpha}n^2}{R} + C_{22}\frac{\bar{\alpha}}{R} + \rho h\omega^2\right]W$$
$$+\left[\kappa^2C_{44}\frac{1}{\ell}\lambda + (\kappa^2C_{45}h - C_{26}\bar{\beta})\frac{n}{Rh}\right]h\Psi + \left[(\kappa^2C_{55}(h-\bar{\beta}) - C_{22}\bar{\beta})\frac{n}{R}\right]h\Phi = 0 \tag{13c}$$

$$\left[-C_{11}\frac{h^3}{12R\ell^2}\lambda^2 - C_{66}\frac{\bar{\beta}n^2}{R} + \rho\frac{h^3\omega^2}{12R}\right]U + \left[-C_{16}\frac{h^3}{12R\ell^2}\lambda^2 - C_{26}\frac{\bar{\beta}n^2}{R} + \kappa^2C_{45}\frac{h}{R}\right]V$$
$$+\left[\kappa^2C_{44}\frac{h}{\ell}\lambda^2 - (C_{26}\bar{\beta} - \kappa^2C_{45}h)\frac{n}{R}\right]W + \left[-C_{11}\frac{h^2}{12\ell^2}\lambda^2 - 2C_{16}\frac{h^2n}{12R\ell}\lambda - C_{66}\frac{\bar{\eta}n^2}{Rh} - \kappa^2C_{44} + \rho\frac{h^2\omega^2}{12}\right]h\Psi$$
$$+\left[-C_{16}\frac{h^2}{12\ell^2}\lambda^2 - (C_{12}+C_{66})\frac{h^2n}{12R\ell}\lambda - C_{26}\frac{\bar{\eta}n^2}{Rh} - \kappa^2C_{45}\right]h\Phi = 0 \tag{13d}$$

$$\left[-C_{16}\frac{h^3}{12R\ell^2}\lambda^2 - C_{26}\frac{\bar{\beta}n^2}{R}\right]U + \left[-C_{66}\frac{h^3}{12R\ell^2}\lambda^2 - C_{22}\frac{\bar{\beta}n^2}{R} + \kappa^2C_{55}\frac{(h-\bar{\beta})}{R} + \rho\frac{h^3\omega^2}{12R}\right]V$$
$$+\left[\kappa^2C_{45}\frac{h}{\ell}\lambda + [\kappa^2C_{55}(h-\bar{\beta}) - C_{22}\bar{\beta}]\frac{n}{R}\right]W + \left[-C_{16}\frac{h^2}{12\ell^2}\lambda^2 - (C_{12}+C_{66})\frac{h^2n}{12R\ell}\lambda\right.$$
$$\left.-C_{26}\frac{\bar{\eta}n^2}{Rh} - \kappa^2C_{45}\right]h\Psi + \left[-C_{66}\frac{h^2}{12\ell^2}\lambda^2 - C_{22}\frac{\bar{\eta}n^2}{Rh} - \kappa^2C_{55}\left(1+\frac{\bar{\eta}}{Rh}\right) + \rho\frac{h^2\omega^2}{12}\right]h\Phi = 0 \tag{13e}$$

Eigenproblem Solution Method

For a given circumferential wave number, n, and angular frequency, ω, we have five homogeneous equations in the five unknown amplitudes. This forms an eigenvalue problem with respect to the axial wave parameter, λ^2. In order to solve for the eigenvalues, we follow the procedure outlined in Ref. 13 wherein we rewrite Eqs. (13) in matrix form as

$$\begin{bmatrix} & & \\ & D & \\ & & \end{bmatrix}\begin{Bmatrix} U \\ V \\ W \\ h\Psi \\ h\Phi \end{Bmatrix} = \begin{Bmatrix} 0 \\ 0 \\ 0 \\ 0 \\ 0 \end{Bmatrix} \tag{14}$$

Here $[D]$ is a so-called lambda matrix defined by

$$[D] \equiv [A^0]\lambda^2 + [A^1]\lambda + [A^2] \tag{15}$$

The components of $[A^0]$, $[A^1]$, and $[A^2]$ can be deduced directly from Eqs. (13). The characteristic roots, λ, in Eq. (15), are the same as those of the standard eigenvalue problem

$$[Z] - \lambda[I] = [0] \tag{16}$$

where here $[Z]$ is the ten-by-ten matrix defined as

$$\begin{bmatrix} Z \end{bmatrix} = \left[\begin{array}{c|c} [0] & [I] \\ \hline [B^2] & [B^1] \end{array}\right] \tag{17}$$

and

$$[B^2] = -[A^0]^{-1}[A^2], \quad [B^1] = -[A^0]^{-1}[A^1] \tag{18}$$

Having found the characteristic values for λ, we see that the complete solution of Eqs. (13), for a given n and ω, is

$$u = \sum_{k=1}^{10} U_k \exp\left[i\left(\frac{\lambda_k x}{\ell} + n\theta - \omega t\right)\right]$$
$$v = \sum_{k=1}^{10} V_k \exp\left[i\left(\frac{\lambda_k x}{\ell} + n\theta - \omega t\right)\right]$$
$$w = \sum_{k=1}^{10} iW_k \exp\left[i\left(\frac{\lambda_k x}{\ell} + n\theta - \omega t\right)\right]$$
$$\psi = \sum_{k=1}^{10} \Psi_k \exp\left[i\left(\frac{\lambda_k x}{\ell} + n\theta - \omega t\right)\right]$$
$$\phi = \sum_{k=1}^{10} \Phi_k \exp\left[i\left(\frac{\lambda_k x}{\ell} + n\theta - \omega t\right)\right] \tag{19}$$

For each value of k (i.e., each eigenvalue, λ) we calculate a set of amplitude (eigenvector) ratios. For the present case, all eigenvectors were normalized by W_k. Since these values are known for each eigenvalue, let a starred quantity designate an appropriate eigenvector ratio. For example,

$$\Psi^*_k = \Psi_k / W_k \tag{20}$$

Then Eqs. (19) can be rewritten in appropriate form and the resulting equations substituted into the boundary conditions, Eqs. (11). Thus, we see that we have a set of ten homogeneous equations in the ten unknown W_k, for a given n and ω. The coefficient matrix for the W_k must be singular in order to have possible solutions to the boundary conditions. An iterative process is then employed on ω, for given n, in order to find the set of eigenvalues and eigenvectors for which the boundary conditions are satisfied. Practically, though, we merely observe a change of sign in the determinant of the coefficient matrix for Eqs. (11). Hence, we may calculate

Table 1 Comparisons among theoretical and experimental resonant frequencies (Hz) for a homogeneous, isotropic, thin cylindrical shell

	First axial mode				Second axial mode			
n	a	b	c	d	a	b	c	d
2	1862.0	1862.0	1862.0	1934.3	3725.0	3725.5	3725.1	3874.0
3	1101.8	1102.0	1101.8	1147.7	2742.6	2743.1	2742.7	2855.8
4	705.7	705.9	705.7	736.3	2018.0	2018.5	2018.1	2103.3
5	497.5	497.7	497.5	520.9	1515.0	1515.4	1515.0	1580.5
6	400.1	400.3	400.1	422.5	1174.9	1175.2	1174.9	1227.7
7	380.7	380.9	380.7	407.0	953.6	953.9	953.7	999.8
8	416.7	416.8	416.7	499.9	824.2	824.6	824.2	869.3
9	488.6	488.7	488.4	532.4	770.4	770.6	770.5	819.2
10	583.9	583.9	583.8	653.9	778.3	778.6	778.5	834.5

Cases: a) Flügge theory from Ref. 14, as listed numerically in Ref. 24; b) experiment from Ref. 14; c) present theory, plane-stress elastic constants; d) present theory, three-dimensional elastic constants. $E = 203$ GN/m^2 (29.5×10^6 psi), $\nu = 0.285$, specific gravity 7.84, $\ell = 29.8$ cm (11.74 in.), $R = 14.8$ cm (5.836 in.), $h = 0.051$ cm (0.020 in.).

resonant frequencies for any shell geometry and for any boundary conditions to any degree of accuracy.

Because the eigenvalues of Eq. (14) are, in general, complex, it is convenient to make another slight alteration in the form of Eqs. (19). This is explained further in Appendices E and F of Ref. 8 where the details of the computer program are described.

IV. Numerical Examples and Comparative Results

Comparison with Previous Investigations

To check the validity of the analytical approach as well as the algebra and programming, comparison with the results obtained by other investigators for special cases is presented. Bray and Egle[14] compared experimental resonant frequencies with those obtained by analysis using Flügge theory, for a homogeneous, isotropic, thin-cylindrical shell. In applying the present analysis to the same shell, two sets of frequencies were obtained. The first set was the result of using the elastic properties from a plane-stress assumption for a thin shell. It can be seen in Table 1 that the comparisons among the Flügge theory, present theory (plane-stress properties), and experiment agree very well.

The second set of frequencies from the present analysis was obtained by using the three-dimensional elastic constants. In all cases the frequencies based on the three-dimensional elastic properties are somewhat higher than the other three. This is consistent with laminated plate results obtained by Wang and Chou.[15] The relative difference between the three-dimensional and two-dimensional results increases as the circumferential wave number increases.

As a second example for use in testing the analysis and programming, consideration is given to a ring-stiffened aluminum shell. Hoppmann[16] analyzed this problem in theory by considering the shell to be specially orthotropic using a hypothetical thickness which lies somewhere between the thickness of the shell and the thickness of the stiffeners. The hypothetical thickness is obtained by experiment. Fairly good comparisons are made for the first axial mode and circumferential modes 2-5 between Hoppmann's experimental and theoretical frequencies and those obtained through the present theory (see Table 2).

It should be noted that axial half-wave numbers are not given explicitly by the present theory. As a result, we refer to the corresponding axial mode as simply the first, second, etc.

The comparative analyses above provide a good check against other analytical methods and experiments for a thin shell. It is desirable to compare the present method against other analytically or experimentally obtained resonant frequencies for a thick shell, since the present theory provides for that case. A search of the literature did not reveal any such examples that were readily adaptable. However, Baker and Herrmann[17] conducted a vibration analysis of a finite-orthotropic cylindrical-sandwich shell which was not thick, in the usual meaning for homogeneous, isotropic shells, but the thickness-shear moduli of the core were so low that thickness-shear deformation must be taken into account.

To adapt the nonhomogeneous sandwich shell to the present analysis, it would be necessary to "smear" the boundary between the core material and the facings, and treat the shell as if it were homogeneous. As a result, a fictitious thickness and density are obtained. Unfortunately, discrepancies were found between Figs. 5 and 6 of Ref. 17, so a quantitative comparison is meaningless. However, the same trend as Fig. 6 of Ref. 17 is obtained when this "equivalent-homogeneous-shell" approach is used.

Table 2 Comparison among fundamental resonant frequencies (Hz) for an orthogonally stiffened thin cylindrical shell modeled as specially orthotropic

n	a	b	c
2	1530	1530	1538
3	4230	4230	4016
4	8100	—	7925
5	13,050	—	12,044

Cases: a) theoretical results from Ref. 16, using Donnell type theory; b) experimental results from Ref. 16; c) present analysis. $\ell = 39.4$ cm (15.53 in.), $R = 5.13$ cm (2.02 in.), $h = 0.48$ cm (0.19 in.), specific gravity, 2.69, elastic compliances: $S_{11} = 0.303$ m^2/GN (2.09×10^{-6} psi^{-1}); $S_{12} = 0.827$ m^2/GN (5.70×10^{-6} psi^{-1}), $S_{22} = 1.294$ m^2/GN (8.92×10^{-6} psi^{-1}), $S_{44} = 0.978$ m^2/GN (6.74×10^{-6} psi^{-1}), $S_{55} = S_{66} = 0.368$ m^2/GN (2.54×10^{-6} psi^{-1}).

Table 3 Resonant frequencies (Hz) for a monoclinic shell with free-free end conditions

Circ. mode Number n	Calculated Lower bound	Upper bound	Experimental
	Fundamental frequencies:		
2	1514	1927	1490, 1580, 1890
3	4211	5209	4100,4290
4	7869	9756	
5	12,320	15,310	10,150
	Second axial mode frequencies:		
2	2117	2587	2400
3	4272	5300	3610
4	7963	9881	
5	12,420	15,450	11,100

$\ell = 13.3$ cm (5.25 in.), $R = 4.14$ cm (1.63 in.), $h = 0.69$ cm (0.27 in.), specific gravity 2.12.

Monoclinic Shell

Figure 2 shows the experimental arrangement used to obtain the free-free end conditions and to detect resonant frequencies. The shell is supported by soft rubber tubing attached to the supporting stand. Since the tubing offers very

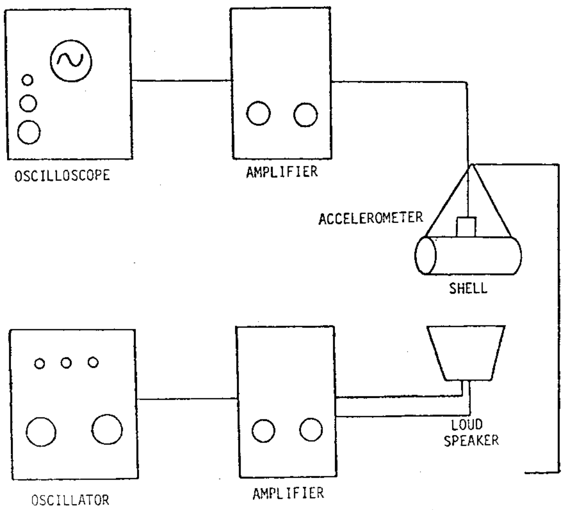

Fig. 2 Experimental arrangement for detecting resonant frequencies.

little resistance to movement in any direction, the end conditions are virtually free-free.

The vibratory motion of the shell was induced by a loudspeaker and consequently, the range of frequencies obtained was restricted to the audio band. An accelerometer was attached to the shell to detect amplitude changes, with the signal then transmitted through an amplifier to an oscilloscope. Resonance was detected as a distinct increase in amplitude.

Unfortunately, this method offers no means of identification of modes with corresponding frequencies. As a result, resonant frequencies cannot be definitely associated with a circumferential wave number. However, to attempt to do so, we assumed that the strong resonances obtained experimentally are associated with the fundamental axial mode, while the medium-response resonances are associated with the second axial mode.

Because of the uncertainty in the values for the transverse Young's modulus, E_2, and in-surface shear modulus, G_{12} (see the Appendix), the high and low cases are compared in Table 3 with the experimentally obtained frequencies.

V. Conclusions

The method of analysis described can be used to obtain a resonant-frequency spectrum for circular-cylindrical shells having wide ranges of geometric parameters (h/R and ℓ/R), material anisotropy, and end conditions. If good initial estimates of resonant frequencies are not available, considerable computing time can be consumed in bracketing and locating the frequencies.

By comparing the experimentally obtained list of frequencies, Table 3, with those obtained by analysis, it appears that the lower moduli provide the more accurate results. Not all of the experimental frequencies are accounted for, however, but this is believed to be due to other higher axial modes not analyzed.

Appendix: Material Constants of Specially Orthotropic Composite Material

Due to the complicated material nature of the cylindrical specimen, it was not possible to determine the material's static-elastic constants by direct measurement without destroying the specimen. Thus, it was necessary to calculate them as described herein.

To calculate the values of the elements in the stiffness matrix used in Eq. (4), we require E_i, G_{ij}, ν_{ij} for an orthotropic system, where i indicates a direction parallel to the fiber direction and i-j represents a plane passing through the fiber direction. Here, E is Young's modulus, G is the shear modulus, and ν is Poisson's ratio.

Let 1 indicate the fiber direction; 2 the in-surface direction normal to the fiber direction; and 3 the radial or thickness direction. An accurate and simple way to calculate E_1, ν_{12} and ν_{13} is by the rule of mixtures,[18] assuming transverse isotropy in the 2-3 plane

$$E_1 = V_f E_f + V_m E_m, \quad \nu_{12} = \nu_{13} = V_f \nu_f + V_m \nu_m \tag{A1}$$

where V_f and V_m are the volume fractions of the constituent fibers and matrix, respectively, and E and ν are the corresponding Young's modulus and Poisson's ratio.

The literature contains calculated values for the transverse Young's modulus that vary considerably about some mean. The same degree of scatter is also true of the longitudinal-transverse shear modulus. Since it was not known, a priori, what effect, if any, a range of these values would have on resonant frequencies, a low and high estimation was used for both moduli. These are not bounding values, in the strict sense, but merely a convenient low and high as found in the literature.[19]

The high value for E_2 $(=E_3)$ and low G_{12} $(=G_{13})$ are taken from Refs. 20 and 21, where the authors graphically displayed the appropriate moduli as functions of constitutent-volume fraction and E_f/E_m and G_f/G_m, respectively. The opposite values given are from Ref. 22, where the author introduced algebraic equations for calculating the stiffness characteristics.

Foye[23] presented a simple equation for calculating the transverse-transverse Poisson's ratio from constituent and known composite moduli as

$$\nu_{23} = V_f \nu_f + V_m \nu_m \left\{ \frac{1+\nu_m - \nu_{12}(E_m/E_1)}{1-\nu_m^2 + \nu_m \nu_{12}(E_m/E_1)} \right\} \tag{A2}$$

where, again, the 1-direction is taken as the longitudinal fiber direction.

The transverse-transverse shear modulus is simply calculated as if the material were isotropic using all transverse values.

$$G_{23} = E_2/[2(1+\nu_{23})] \tag{A3}$$

The elements of the three-dimensional elastic stiffness matrix for an orthotropic medium were given by Jones[18] as

$$C_{11} = \frac{1-\nu_{23}\nu_{32}}{E_2 E_3 \Delta} \qquad C_{22} = \frac{1-\nu_{13}\nu_{31}}{E_1 E_3 \Delta}$$

$$C_{12} = \frac{\nu_{21}+\nu_{31}\nu_{23}}{E_2 E_3 \Delta} \qquad C_{23} = \frac{\nu_{32}+\nu_{12}\nu_{31}}{E_1 E_3 \Delta}$$

$$C_{13} = \frac{\nu_{31}+\nu_{21}\nu_{32}}{E_2 E_3 \Delta} \qquad C_{33} = \frac{1-\nu_{12}\nu_{21}}{E_1 E_2 \Delta}$$

$$C_{44} = G_{23} \qquad C_{55} = G_{31} \qquad C_{66} = G_{12} \tag{A4}$$

where

$$\Delta = \frac{1-\nu_{12}\nu_{21}-\nu_{23}\nu_{32}-\nu_{31}\nu_{13}-2\nu_{21}\nu_{32}\nu_{13}}{E_1 E_2 E_3} \tag{A5}$$

We also use the well-known relation

$$\nu_{ij}/E_i = \nu_{ji}/E_j \tag{A6}$$

The shell investigated in the present analysis was estimated to have the following properties.

Fiber (S-glass): $E_f = 82.7$ GN/m^2 (12×10^6 psi), $G_f = 33.1$ GN/m^2 (4.8×10^6 psi), $\nu_f = 0.25$, $V_f = 0.725$, specific gravity 2.48;

Matrix (epoxy): $E_m = 3.17$ GN/m^2 (4.6×10^5 psi), $G_m = 1.31$ GN/m^2 (1.9×10^5 psi), $\nu_m = 0.35$, $V_m = 0.275$, specific gravity 1.19;

Composite (orthotropic):

$$E_1 = 61.2 \text{ GN/m}^2 \ (8.87 \times 10^6 \text{ psi})$$

$$E_2 = E_3 = \begin{cases} 25.4 \text{ GN/m}^2 \ (3.68 \times 10^6 \text{ psi}) \text{ (high)} \\ 15.1 \text{ GN/m}^2 \ (2.19 \times 10^6 \text{ psi}) \text{ (low)} \end{cases}$$

$$G_{12} = G_{13} = \begin{cases} 10.1 \text{ GN/m}^2 \ (1.46 \times 10^6 \text{ psi}) \text{ (high)} \\ 9.17 \text{ GN/m}^2 \ (1.33 \times 10^6 \text{ psi}) \text{ (low)} \end{cases}$$

$$G_{23} = 9.58 \text{ GN/m}^2 \ (1.39 \times 10^6 \text{ psi})$$

$$\nu_{12} = \nu_{13} = 0.28, \ \nu_{21} = \nu_{31} = 0.07, \ \nu_{23} = \nu_{32} = 0.33$$

The resulting elastic stiffnesses become for the high-modulus orthotropic material

$$C_{11} = 64.8 \text{ GN/m}^2 \ (9.4 \times 10^6 \text{ psi})$$

$$C_{12} = C_{13} = 6.62 \text{ GN/m}^2 \ (0.96 \times 10^6 \text{ psi})$$

$$C_{22} = C_{33} = 29.6 \text{ GN/m}^2 \ (4.3 \times 10^6 \text{ psi})$$

$$C_{23} = 10.3 \text{ GN/m}^2 \ (1.5 \times 10^6 \text{ psi})$$

$$C_{44} = 9.65 \text{ GN/m}^2 \ (1.4 \times 10^6 \text{ psi})$$

$$C_{55} = C_{66} = 8.96 \text{ GN/m}^2 \ (1.3 \times 10^6 \text{ psi})$$

The properties given above are the best available for the test specimen. Simple tests were conducted for estimating V_f and ρ, and the material properties were taken from the literature without test, since only a limited amount of the specially-made monoclinic material was available.

Acknowledgments

The research reported here is based upon a thesis submitted by the first author in partial fulfillment of the requirements for the M.S. degree in Mechanical Engineering at the University of Oklahoma, Norman, Okla., Dec. 1978. Computing time was provided by the University's Merrick Computing Center.

References

[1] Leissa, A. W., "Vibration of Shells," NASA SP-228, 1973.

[2] Bert, C. W. and Egle, D., "Dynamics of Composite, Sandwich and Stiffened Shell-Type Structures," *Journal of Spacecraft and Rockets*, Vol. 6, Dec. 1969, pp. 1345-1361.

[3] Bert, C. W. and Francis, P. H., "Composite Material Mechanics: Structural Mechanics," *AIAA Journal*, Vol. 12, Dec. 1974, pp. 1173-1186.

[4] Love, A.E.H., "On the Small, Free Vibrations and Deformation of a Thin Elastic Shell," *Philosophical Transactions of the Royal Society*, London, England, Series A, Vol. 179, 1888, pp. 491-546.

[5] Mirsky, I., "Vibrations of Orthotropic, Thick, Cylindrical Shells," *Journal of the Acoustical Society of America*, Vol. 36, Jan. 1964, pp. 41-51.

[6] Forsberg, K., "Influence of Boundary Conditions on the Modal Characteristics of Thin Elastic Shells," *AIAA Journal*, Vol. 2, Dec. 1964, pp. 2150-2157.

[7] Kraus, H., *Thin Elastic Shells*, John Wiley and Sons, New York, 1967.

[8] Vanderpool, M. E., "Free Vibrations of a Materially Monoclinic, Thick-Wall, Circular Cylindrical Shell," M.S. Thesis, Mechanical Engineering, University of Oklahoma, Norman, Okla., Dec. 1978.

[9] Cooper, R. M. and Naghdi, P. M., "Propagation of Non-Axially Symmetric Waves in Elastic Cylindrical Shells," *Journal of the Acoustical Society of America*, Vol. 29, Dec. 1957, pp. 1365-1373.

[10] Mindlin, R. D., "Influence of Rotatory Inertia and Shear on Flexural Motions of Isotropic, Elastic Plates," *Journal of Applied Mechanics*, Vol. 18, March 1951, pp. 31-38.

[11] Langhaar, H. L. and Boresi, A. P., "Strain Energy and Equilibrium of a Shell Subjected to Arbitrary Temperature Distribution," *Proceedings of 3rd U.S. National Congress of Applied Mechanics*, 1958, pp. 393-399.

[12] Flügge, W., *Stresses in Shells*, 2nd Ed., Springer-Verlag, New York, 1973, Chap. 8.

[13] Gourlay, A. R. and Watson, G. A., *Computational Methods for Matrix Eigenproblems*, John Wiley and Sons, New York, 1973, Chap. 14.

[14] Bray, F. M. and Egle, D. M., "An Experimental Investigation of the Free Vibration of Thin Cylindrical Shells with Discrete Longitudinal Stiffening," *Journal of Sound and Vibration*, Vol. 12, June 1970, pp. 153-164.

[15] Wang, A.S.D. and Chou, P. C., "A Comparison of Two Laminated Plate Theories," *Journal of Applied Mechanics*, Vol. 39, June 1972, pp. 611-613.

[16] Hoppmann, W. H., "Some Characteristics of the Flexural Vibrations of Orthogonally Stiffened Cylindrical Shells," *Journal of the Acoustical Society of America*, Vol. 30, Jan. 1958, pp. 77-82.

[17] Baker, E. H. and Herrmann, G., "Vibrations of Orthotropic Cylindrical Sandwich Shells under Initial Stress," *AIAA Journal*, Vol. 4, June 1966, pp. 1063-1070.

[18] Jones, R. M., *Mechanics of Composite Materials*, McGraw-Hill, New York, 1975.

[19] Chamis, C. C. and Sendeckyj, G. P., "Critique on Theories Predicting Thermoelastic Properties of Fibrous Composites," *Journal of Composite Materials*, Vol. 2, July 1968, pp. 332-358.

[20] Adams, D. F. and Doner, D. R., "Longitudinal Shear Loading of a Unidirectional Composite," *Journal of Composite Materials*, Vol. 1, Jan. 1967, pp. 4-17.

[21] Adams, D. F. and Doner, D. R., "Transverse Normal Loading of a Unidirectional Composite," *Journal of Composite Materials*, Vol. 1, April 1967, pp. 152-164.

[22] Ekvall, J. C., "Structural Behavior of Monofilament Composites," *AIAA 6th Structures and Materials Conference*, Palm Springs, Calif., April 1965, pp. 250-263.

[23] Foye, R. L., "The Transverse Poisson's Ratio of Composites," *Journal of Composite Materials*, Vol. 6, April 1972, pp. 293-295.

[24] Bert, C. W., Baker, J. L., and Egle, D. M., "Free Vibrations of Multilayer Anisotropic Cylindrical Shells," *Journal of Composite Materials*, Vol. 3, July 1969, pp. 480-499.